Effect of Non-Metallic Inclusions on the Hot Ductility of High-Mn Steels

Marek Opiela[1*], Gabriela Fojt-Dymara[2]

[1] Faculty of Mechanical Engineering, Department of Engineering Materials and Biomaterials, Silesian University of Technology, ul. Konarskiego 18A, 44-100 Gliwice, Poland

[2] Faculty of Mechanical Engineering, Department of Engineering Processes Automation and Integrated Manufacturing Systems, Silesian University of Technology, ul. Konarskiego 18A, 44-100 Gliwice, Poland

* Corresponding author's e-mail: marek.opiela@polsl.pl

ABSTRACT

The aim of the work was to determine the effect of non-metallic inclusions on the hot ductility of two newly developed high-Mn austenitic steels (27Mn-4Si-2Al and 24Mn-3Si-1.5Al-Ti). For this purpose, a hot tensile test was carried out in the temperature range from 1050°C to 1200°C with a constant strain rate of $2.5 \cdot 10^{-3}\,s^{-1}$. The tests were performed on the Gleeble 3800 thermomechanical simulator. Hot ductility of tested steels was defined by determining the reduction in area (% RA). Examined steels demonstrate diversified hot ductility. Clearly higher hot ductility was noted for the 24Mn-3Si-1.5Al-Ti steel. The reduction in area of this steel in the temperature range from 1050°C to 1200°C decreases from approx. 90% to about 58%, while the reduction in area of the 27Mn-4Si-2Al steel, in the same temperature range, decreases from approx. 66% to about 34%. The presence of single, regular-shaped AlN particles and complex MnS-AlN-type non-metallic inclusions was revealed in the 27Mn-4Si-2Al steel. Whereas fine (Ce, La, Nd)S-type sulphides, properly modified with rare earth elements, were identified in the 24Mn-3Si-1.5Al-Ti steel. The AlN-type inclusions and complex MnS-AlN-type inclusions were not revealed in the 24Mn-3Si-1.5Al-Ti steel. This is due to the presence of Ti microaddition, the concentration of which guaranteed binding of the whole nitrogen into stable TiN-type nitrides. Sulphides, disclosed in the 24Mn-3Si-1.5Al-Ti steel, are globular or slightly elongated in the direction of plastic deformation, as confirmed by a very low value of the elongation factor equal 1.48. This creates the opportunity to produce sheets of high strength and ductility and low anisotropy of mechanical properties.

Keywords: non-metallic inclusions, hot ductility, high manganese steels, mechanical properties.

INTRODUCTION

The automotive industry is one of the most developing industries, in terms of technology and the types of materials used to build the car body [1]. Despite growing tendency to use low-density alloys in the automotive industry, e.g. aluminium and magnesium based as well as polymer or composite materials, yet more than 60% of the car weight are constructional elements, formed from steel sheets with increasing strength, good plasticity and susceptibility to pressing [2, 3].

One of the groups of steels, assuring high application potential for structural components in the automotive industry, are high-manganese austenitic steels [4, 5]. These steels, characterized by high strength properties (UTS = 600÷900 MPa, $YS_{0.2}$ = 250÷450 MPa), plastic properties (El = 35÷80%) and reduced density (ρ = 7,3 g/cm³), can be applied to produce car body elements which demonstrate the ability to absorb large amount of energy during dynamic deformation, improving the safety of passengers [6, 8]. High mechanical properties of this group of steels depend on the chemical composition, in particular on Mn concentration (from 15% to 30%), which determines the main strengthening mechanism during technological forming [9]. High hardening rate of these steels and good plasticity result from strain-induced martensitic transformation [10–12] or

mechanical twinning [13–15]. The problem for wider use of this group of steels is insufficient hot ductility – especially above 1100°C [16–18] – and susceptibility to initiation and propagation of cracks in the surface layer of the ingot obtained with the use of continuous casting [19, 20].

One of the reasons for decreased high-temperature ductility and intercrystalline embrittlement of high-Mn steels is the presence of non-metallic inclusions; this impact is determined by their morphology and chemical composition.

Park et al. [21] revealed that the following types of non-metallic inclusions can be distinguished in the Fe-Mn-Al-type high-manganese steels: Al_2O_3, AlN, $MnAl_2O_4$, Al_2O_3-AlN, MnS, Al_2O_3-MnS, MnS-AlN, and that the greatest fraction of non-metallic inclusions is present when the Al content is equal 3%. The influence of non-metallic inclusions on high-temperature ductility in Fe-16Mn-xAl-0.6C type steels with diversified Al concentration (x = 0.002%, 0.033%, 0.54% and 2.10%) was the subject of research carried out by Wang et al. [22]. Performed tests showed that with the increase of the Al content in steel, chemical composition of the dominant non-metallic inclusions changed as follows: MnO → Al_2O_3-MnS → MnS → AlN. It was also revealed in the work that high-temperature ductility of steel, containing 0.033% Al, is about 30% higher comparing to other steels. The addition of Al in steels with high content of Mn reduces density [23, 24], increases stacking fault energy [25], wherein AlN-type precipitations may cause intercrystalline cracks [26–29]. Liu et al. [16] examined the impact of Mn (15%, 18% and 24%) and Al (0.002%, 0.75% and 1.47%) concentration on hot ductility. Conducted research revealed that the highest hot ductility was found for steel containing 0.002% Al. The microstructure and flow curves indicated the course of dynamic recrystallization. The amount of recrystallized grains rapidly decreased with the increase of Mn concentration. Greater portion of AlN particles was observed along with increasing concentration of Al. Large portion of these particles, present mainly on the boundaries of austenite grains, caused the inhibition of the dynamic recrystallization process, which disadvantageously affected hot ductility. Similar results were observed in [30, 31]. Research on the effect of Ti and B microadditions on hot ductility of high-manganese steel was carried out by Mejia et al. [17]. Uniaxial hot tensile tests (700÷1100°C) were done at the rate of $1·10^{-3}$ s^{-1}. They demonstrated that the ongoing dynamic recrystallization in the examined temperature range has advantageous impact on hot ductility. Moreover, they found that the Ti microaddition, bonding with nitrogen into TiN, prevents the precipitation of AlN and BN-type nitrides, which affect the decrease of hot ductility. The impact of Ti on increase of hot ductility in high-Mn steels was also presented by Abushosha et al. [32]. The authors observed that the Ti microaddition, precipitating on grain boundaries in the form of fine TiN precipitations, leaves smaller voids when comparing to those caused by larger and more damaging AlN precipitations. The effect of AlN-type nitrides on hot ductility depends also on the concentration of S in steel [33, 34]. In steels with high concentration of S, AlN particles indirectly contribute to the decrease of hot ductility by bonding with previously precipitated MnS-type sulphides. Mintz, Qaban et al. showed that steels with low sulphur content (S < 0.005%) have high hot ductility, and AlN-type nitrides precipitate both on grain boundaries and in the matrix. Similar conclusions were reached in [22]. It has been revealed that in high-manganese steels, containing less than 0.005% S, uniform precipitation of AlN-type nitrides in the matrix and on grain boundaries does not affect the propagation of cracks during the ingot straightening operation. The aim of the work is to investigate the effect of non-metallic inclusions on the hot ductility of newly developed high-Mn steels.

MATERIALS AND METHODS

The tests were carried out on two newly developed grades of C-Mn-Si-Al type high-manganese steel with the chemical composition presented in Table 1. Melts were done in a VSG-100 type laboratory vacuum induction furnace. Tested steels are characterized by limited concentration of P, S and gases (the concentration of oxygen was determined by the high-temperature extraction method), high concentration of Mn and increased concentration of Si and Al. Silicon significantly inhibits the process of carbides formation during bainitic transformation [35, 36]. However, this element causes deterioration of the surface quality of sheet in the rolling process and impairs the wettability of the sheet by liquid zinc in the galvanization process [37]. Aluminium, in turn, reduces precipitation of cementite [38]. Diversified

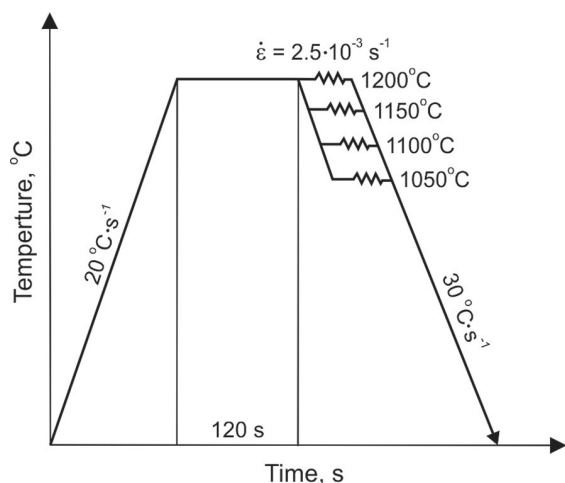**Table 1.** Chemical composition of investigated steels

27Mn-4Si-2Al								
C	Mn	P	S	Si	Al	Ti	N	O
0.040	27.4	0.002	0.018	4.0	2.0	–	0.0028	0.0007
24Mn-3Si-1.5Al-Ti								
C	Mn	P	S	Si	Al	Ti	N	O
0.055	24.4	0.004	0.016	3.4	1.5	0.075	0.0040	0.0006

concentration of Si and Al determines that examined steels have different values of austenite stacking fault energy (27.3 mJ·m^2 and 18.9 mJ·m^2 – 27Mn-4Si-2Al and 24Mn-3Si-1.5Al-Ti steel, respectively), and thus diverse susceptibility to martensitic transformation or mechanical twinning during cold working. Introduction of Ti microaddition to the 24Mn-3Si-1.5Al-Ti steel should ensure bonding of the whole nitrogen into stable TiN-type nitrides. Modification of non-metallic inclusions in the melt with Ti microaddition was carried out using rare earth elements (~50% Ce, ~50% La, ~20% Nd) in the amount of 8 g per 1 kg of steel.

The melts, weighing 26 kg, were subjected to initial hot working. After austenitizing at the temperature of 1200°C the ingots were subjected to free forging on a hydraulic press. The forging finish temperature was equal 900°C. Produced flat bars, measuring 20 mm × 220 mm, were successively subjected to hot rolling. After austenitizing for 1200 s at the temperature of 1100°C, the flat bars were rolled in four passes (1050°C, 1000°C, 950°C and 900°C) using a 25% reduction ratio in the first two passes, and a 20% reduction ratio in the last two passes. In this way, 6.5 mm thick sheet was produced from which samples (ϕ 6 mm

x 116.5 mm) were obtained to be used in high-temperature tensile test.

Hot tensile tests were carried out using the Gleeble 3800 compression plastometer – equipment available in the Scientific and Didactic Laboratory of Nanotechnology and Material Technologies of the Silesian University of Technology. The samples were resistance heated at the rate of 20°C·s^{-1} to the austenitizing temperature of 1200°C. After heating at this temperature for 120 s, the specimens were cooled at the rate of 5°C·s^{-1} to the temperature of plastic deformation (1150°C, 1100°C, 1050°C) and heated for 30 s before deformation. For comparison, one of the samples was subjected to tension immediately after heating at the temperature of 1200°C. The samples were stretched under vacuum to fracture at a constant strain rate of 2.5·10^{-3} s^{-1}. After deformation, the specimens were cooled to ambient temperature at the rate of 30°C·s^{-1}. The test temperature was controlled with the use of thermocouples welded to the samples. Three tests were performed for each deformation program. The research program is schematically presented in Figure 1. Hot ductility of investigated steels as a function of temperature was defined by determining the reduction in area (% RA).

With the aim to evaluate the correctness of the metallurgical process in terms of contamination degree of steel with non-metallic inclusions, as well as to confirm carried out modification of non-metallic inclusions with rare earth elements, the portion, type and morphology of these inclusions were determined. Evaluation of the degree of contamination of tested steels with non-metallic inclusions was performed on non-etched specimens, using LEICA MEF 4A light microscope, in the magnification range of 100÷500x. The surface area of inclusions, their surface area fraction and elongation factor were determined. Chemical composition of non-metallic inclusions, revealed near the fracture, was determined using EDAX TRIDENT XM4 EDS X-ray energy spectrometer,

Figure 1. Scheme of hot tensile tests

which is an integral part of the SUPRA 35 high-resolution scanning microscope.

RESULTS

Hot tensile tests of the investigated steels, performed in the temperature range from 1050°C to 1200°C at a constant strain rate of $2.5 \cdot 10^{-3}$ s^{-1}, allowed to determine the effect of the test temperature on mechanical properties. As expected, along with the decrease in temperature, there was an increase in the strength and the value of deformation e$_{max}$, corresponding with the maximum value of yield stress. In the tensile temperature range from 1200°C to 1050°C, the strength of the 27Mn-4Si-2Al steel increased from approx. 10 MPa to about 30 MPa, while the deformation value e$_{max}$ increased from approx. 0.015 to approx. 0.095. In the examined temperature range, the 24Mn-3Si-1.5Al-Ti steel demonstrates higher values of the maximum yield stress σ$_{max}$ compared to the 27Mn-4Si-2Al steel. Decrease of plastic deformation temperature leads to increase in the maximum yield stress from approx. 16 MPa to about 45 MPa. Detailed data on the hot tensile

test are summarized in Table 2. The hot ductility of investigated high-manganese steels was determined based on the evaluation of the reduction in area (% RA). The influence of plastic strain temperature and chemical composition on the changes of the reduction in area is shown in Figure 2. The data set together in this figure reveal that, in the entire test temperature range, the 24Mn-3Si-1.5Al-Ti steel shows clearly higher reduction in area values compared to the 27Mn-4Si-2Al steel. The reduction in area of the 24Mn-3Si-1.5Al-Ti steel samples decreases from approx. 90% at the temperature of 1050°C to about 58% at the temperature of 1200°C. The reduction in area of the 27Mn-4Si-2Al steel, subjected to tension in the same temperature range, decreases from approx. 66% to about 34%.

Quantitative analysis of non-metallic inclusions made it possible to define main stereological parameters, i.e. the quantity of inclusions per 1 mm^2, their portion, the average surface area and the coefficient characterizing susceptibility of the inclusions to elongate in the direction of plastic working. Performed research revealed numerous non-metallic inclusions in the 27Mn-4Si-2Al steel, often elongated in the direction of plastic

Table 2. The results of the effect of the temperature of plastic deformation on the mechanical properties of the ivestigated steels

Steel designation	27Mn-4Si-2Al			24Mn-3Si-1.5Al-Ti		
Temperature of plastic deformation, °C	σ$_{max}$, MPa	ε$_{max}$	RA, %	σ$_{max}$, MPa	ε$_{max}$	RA, %
1050	30±5	0.095±0.021	66±4	45±7	0.110±0.012	90±3
1100	22±7	0.084±0.016	58±5	28±4	0.081±0.022	86±5
1150	17±6	0.065±0.018	50±4	23±3	0.072±0.015	76±2
1200	10±3	0.015±0.010	34±5	16±2	0.050±0.008	58±6
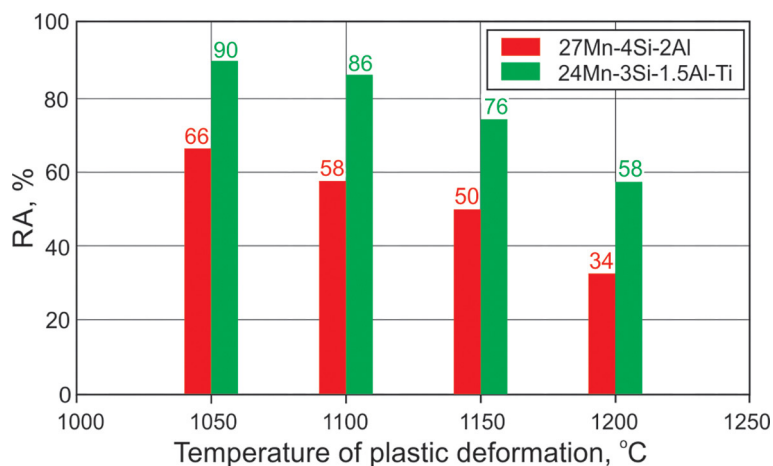
Figure 2. Effect of the temperature of plastic deformation on the reduction of area of the tested steels

working (Fig. 3a). Basing on the data presented in Table 3 and the histograms presented in Figure 4, it can be concluded that the average quantity of non-metallic inclusions per 1 mm^2 in the 27Mn-4Si-2Al steel is approx. 53, and their average surface area fraction is approx. 0.11%. In most cases, small non-metallic inclusions with average surface area of approx. 40 mm^2 were identified in the tested steel. Revealed non-metallic inclusions were most often of a regular form, clearly elongated in the direction of plastic working, as evidenced by high value of the elongation coefficient of approx. 3. The 24Mn-3Si-1.5Al-Ti steel demonstrates lower degree of contamination with non-metallic inclusions (Fig. 3b). Based on performed quantitative analysis, it was found that this steel contains on average about 36 non-metallic inclusions per 1 mm^2 of the microsection surface.

The average surface area of revealed non-metallic inclusions is approx. 23 mm^2, while the surface area fraction of the inclusions is only 0.072%. Noteworthy is the small value of the elongation factor, i.e. the ratio of the inclusion length to its thickness, equal 1.48.

The morphology and chemical composition of non-metallic inclusions revealed in the 27Mn-4Si-2Al steel (on the longitudinal sections near the sample fracture) are shown in Figure 5-7. Conducted analysis showed the presence – in the majority of cases – of single regular-shaped AlN particles and complex MnS-AlN-type non-metallic inclusions. The presence of MnS-type inclusions was noted in the 27Mn-4Si-2Al steel incidentally. According to the data compiled in [33, 39], MnS-type non-metallic inclusions are convenient for precipitation of AlN-type particles. Precise
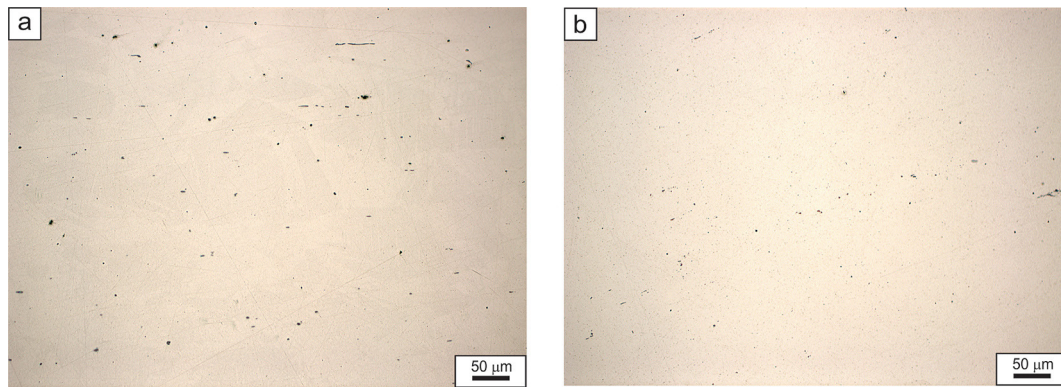

Figure 3. Fine non-metallic inclusions on the longitudinal section of the steel sample: (a) 27Mn-4Si-2Al, (b) 24Mn-3Si-1.5Al-Ti
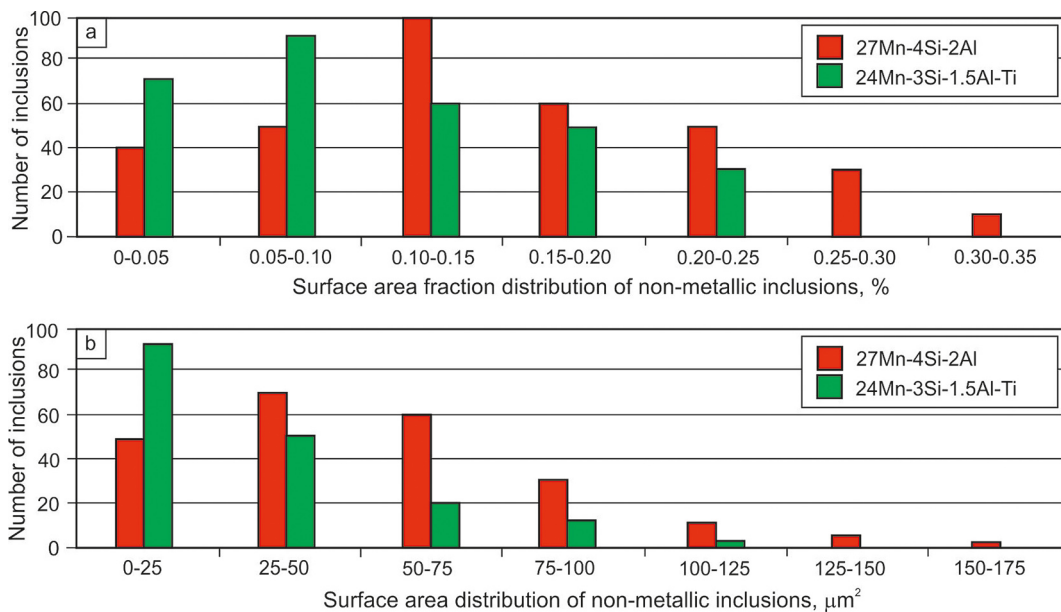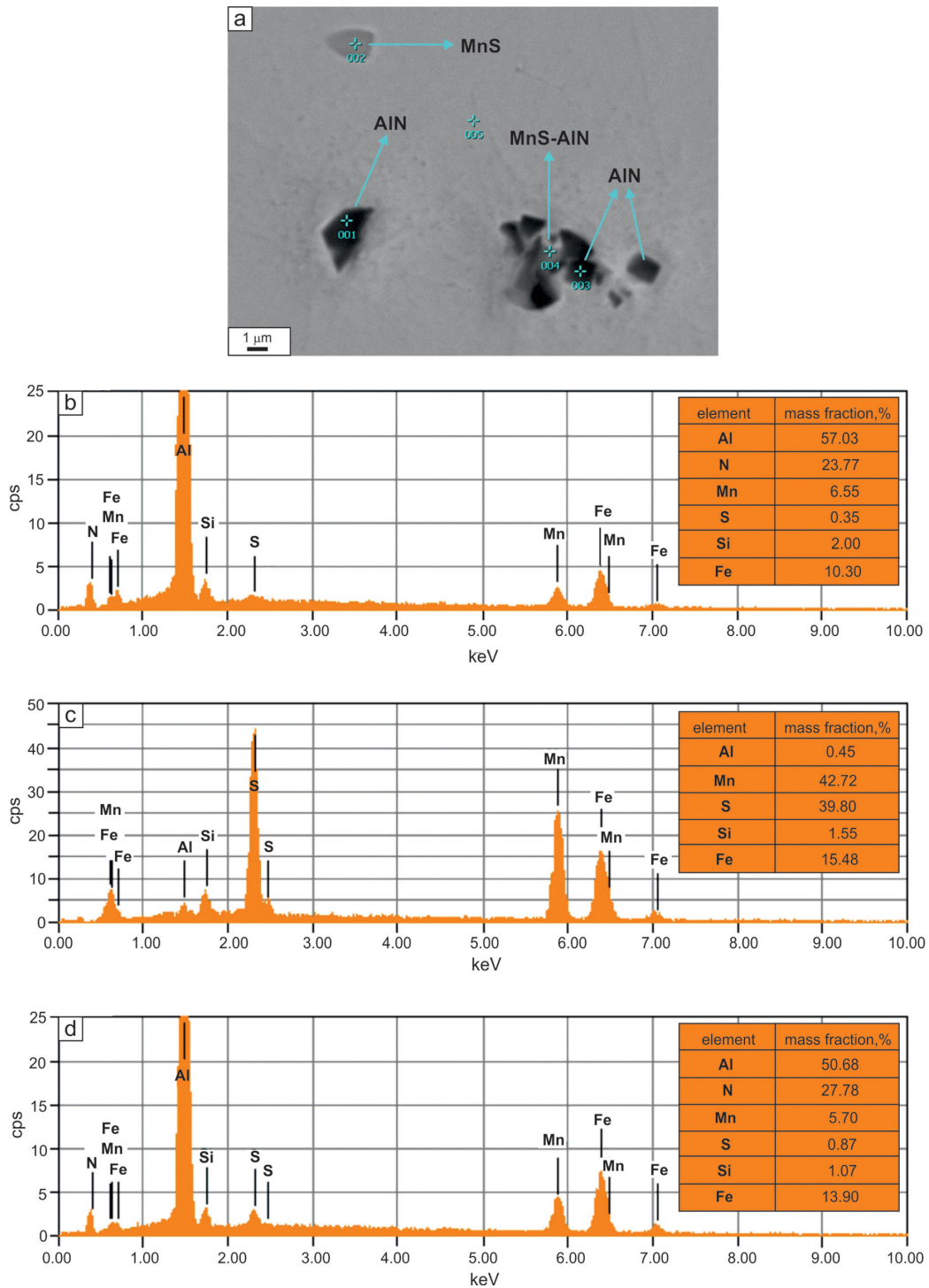

Figure 4. Surface area fraction distribution of non-metallic inclusions (a) and their area (b)
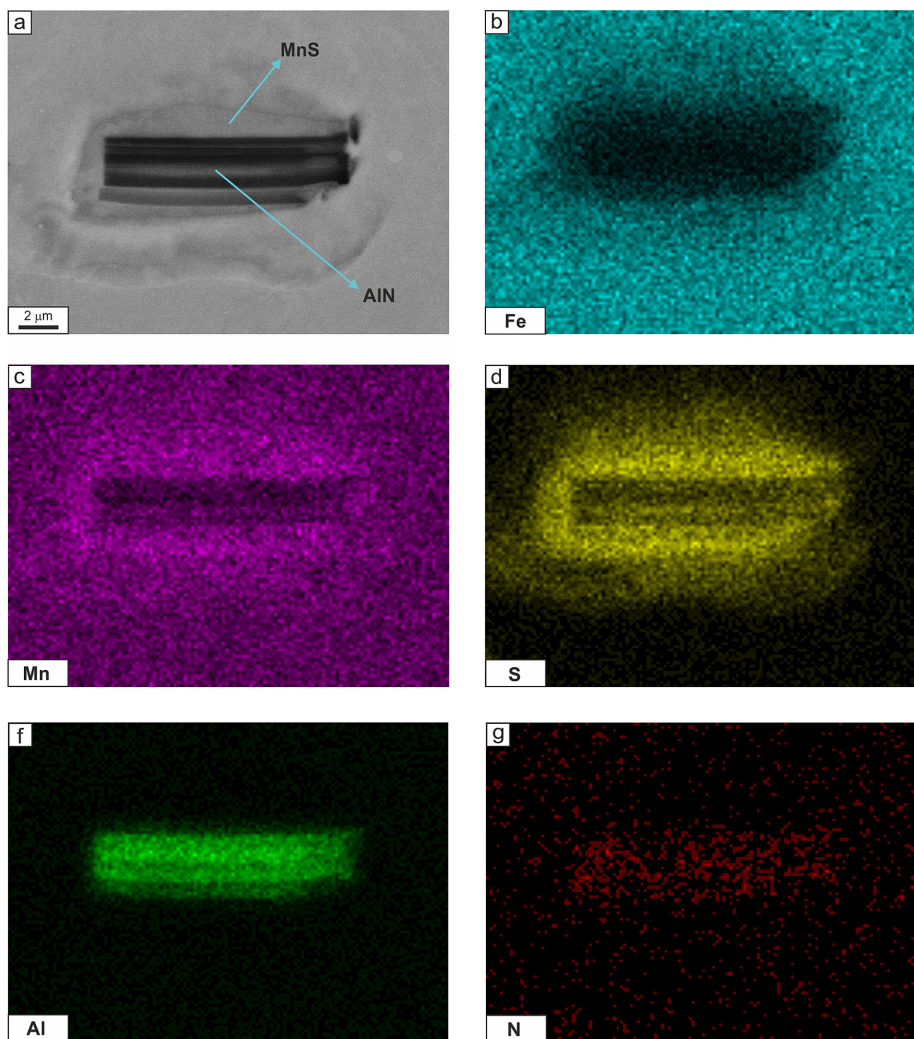
Figure 5. Non-metallic inclusions AlN, MnS-AlN and MnS type: (a) view of particles, (b–d) – spectrum from points 1, 2 and 3 respectively; temperature of plastic deformation: 1100°C; steel 27Mn-4Si-2Al

location of individual elements can be observed in the maps of distribution of elements included in the composition of studied inclusion. They confirm the presence of Al and N in the central part of the inclusion and the presence of Mn and S halo-like form around the AlN particle (Fig. 7). Qualitative analysis of chemical composition of non-metallic inclusions in the 24Mn-3Si-1.5Al-Ti

steel indicates the effectiveness of applied modification of non-metallic inclusions with rare earth elements during the melting process. It was confirmed in the spectrograms of investigated non-metallic inclusions, where in addition to spectral lines deriving from Mn, S, Al, Si and Fe, there are also spectral lines coming from Ce, La and Nd. In the examined 24Mn-3Si-1.5Al-Ti steel, in
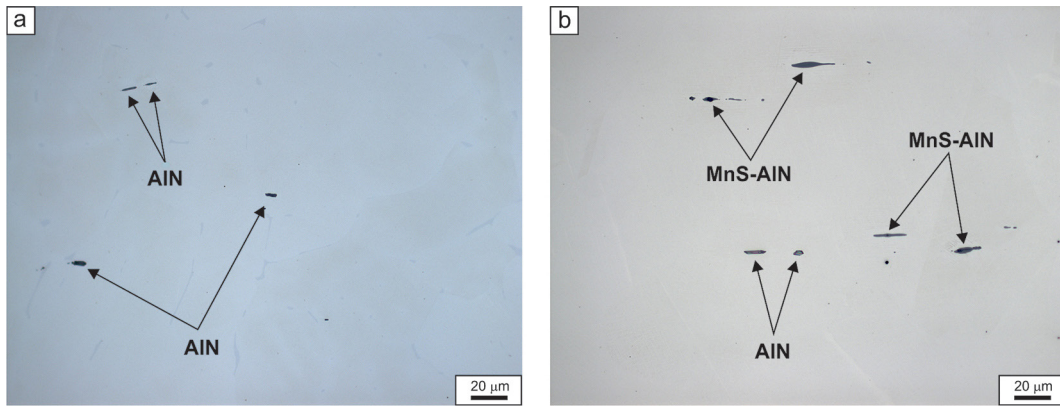
Figure 6. View of AlN-type particles (a) and complex MnS-AlN-type inclusions, (b) temperature of plastic deformation: 1050 °C i 1200°C respectively; steel 27Mn-4Si-2Al

Figure 7. A complex non-metallic inclusion of the MnS-AlN-type: (a) view of the inclusion, (b–g) – distribution maps of elements; temperature of plastic deformation: 1150°C; steel 27Mn-4Si-2Al

the vast majority, fine, globular or slightly elongated in the direction of plastic flow (Ce, La, Nd) S-type sulphides were revealed, in which manganese was almost completely displaced by rare earth elements (Fig. 8). The presence of spectral lines deriving from Fe, Mn, Al and Si in spectrograms is a result of analysing also a certain part of the matrix surrounding non-metallic inclusions.
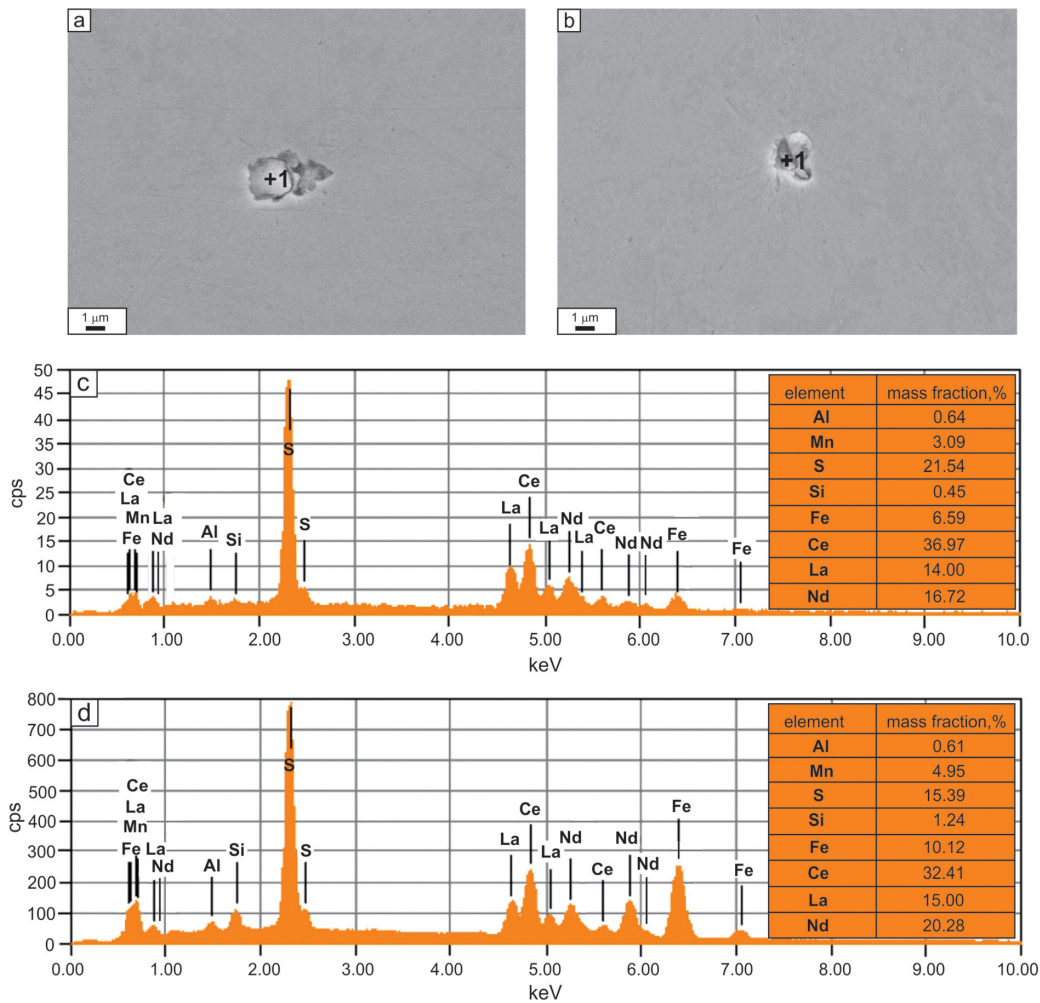
Figure 8. Non-metallic inclusions (Ce, La, Nd)S-type: (a, b) view of particles, (c, d) spectra of the inclusions; temperature of plastic deformation: 1050°C i 1200°C; steel 24Mn-3Si-1.5Al-Ti
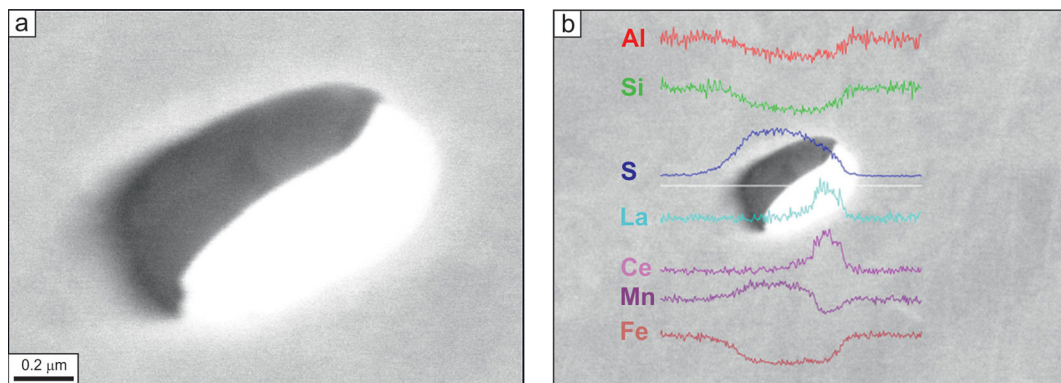
Figure 9. Partially modified non-metallic inclusions of the MnS-type with rare earth elements: (a) view of particle, (b) linear distribution of elements; temperature of plastic deformation: 1150 °C; steel 24Mn-3Si-1.5Al-Ti

Displacement of Mn from sulphide inclusions by Ce, La and Nd proves almost complete modification of these inclusions. It's the result of rare earth elements forming more stable sulphides than MnS. High stability of rare earth sulphides is due to their high melting point. As per example, the melting point of Ce_2S_3, La_2S_3 and Nd_2S_3 sulphides is equal 2150°C, 2099°C and 2199°C respectively, while the melting point of MnS is equal 1539°C [40]. In a few cases, non-metallic inclusions partially modified with rare earth elements were revealed (Fig. 9). Visible darker inclusion area in Figure 9a

is the unmodified part of the MnS-type sulphide. The results of the linear analysis (Fig. 9a) indicate distinct increase in concentration of La and Ce, visible in the brighter area of the inclusion, with simultaneous decrease of Mn concentration in this part of the inclusion. Due to low oxygen concentration (0.0007% and 0.0006% in the 27Mn-4Si-2Al and 24Mn-3Si-1.5Al-Ti steel, respectively), oxide inclusions were practically not observed.

DISCUSSION

Conducted research of hot ductility revealed that the 24Mn-3Si-1.5Al-Ti steel has higher values of the reduction in area in the entire temperature range (Fig. 2). This should be connected to lower concentration of Al and the presence of Ti microaddition, which, showing high chemical affinity to nitrogen, bonds with this element into stable TiN-type nitrides, thus preventing the formation of AlN-type nitrides that are damaging to the ductility [41, 42]. The analysis of literature references indicates limited studies on the ductility of high-Mn steels at temperatures above 1100°C [16, 43]. In most cases, the results of ductility tests presented in these works concern the temperature range from 700°C to 1100°C. Table 4 shows ductility results of selected high-manganese steels with various chemical composition at the temperature of 1100°C – which is the highest test temperature in the cited works [16-18, 33, 43]. Basing on the data presented in this table, the reduction in area of the samples at the temperature of 1100°C – depending on the chemical composition – varies from 8% to 38%. High-manganese

steels, studied as part of the work, demonstrate reduction in area values of approximately 58% and about 86% – for 27Mn-4Si-2Al and 24Mn-3Si-1.5Al-Ti, respectively. Therefore, comparing the reduction in area values of tested steels (Table 2) with the values presented in Table 4, obtained results of hot ductility should be considered satisfactory, especially in case of steel with Ti microaddition, i.e. 24Mn-3Si-1.5Al-Ti.

Performed evaluation of contamination degree of investigated high-Mn steels with non-metallic inclusions showed that they are of similar content (Table 3, Fig. 3) but can be distinguished by different morphology and chemical composition. Figure 3 shows only one of the many areas taken into account for the computer analysis of non-metallic inclusions. Of course, the entire area visible in this figure is significant, and thus all non-metallic inclusions present there were taken into account for quantitative assessment. The results listed in Table 3 are the average of the analysis of 10 different areas for each steel. The 27Mn-4Si-2Al steel is characterized primarily by the presence of AlN-type precipitations (Fig. 5a and Fig. 6a) and complex MnS-AlN-type inclusions (Fig. 5-7). The chemical composition and morphology of non-metallic inclusions revealed in the 27Mn-4Si-2Al steel are consistent with those presented by Wang et al. in [22], where the effect of AlN on the hot ductility of austenitic steel with similar chemical composition was examined. The presence of AlN and MnS-AlN-type inclusions in the 27Mn-4Si-2Al steel impacts the decrease of hot ductility and may be the cause of intergranular embrittlement [33, 44]. Whereas globular non-metallic inclusions with high dispersion were

Table 3. Quantitative analysis of non-metallic inclusions of the investigated high-Mn steels

27Mn-4Si-2Al			
Parameters of the non-metallic inclusions	Minimum value	Maksimum value	Average value
Number of inlusions, mm^{-2}	14.70	112.30	53.19
Surface fraction, %	0.04	0.32	0.110
Inclusions surface, μm^2	7.55	160.12	39.50
Elongation coefficient, l/s*	1.20	8.70	3.02
24Mn-3Si-1.5Al-Ti			
Parameters of the non-metallic inclusions	Minimum value	Maksimum value	Average value
Number of inlusions, mm^{-2}	8.15	80.65	36.20
Surface fraction, %	0.02	0.23	0.072
Inclusions surface, μm^2	3.65	119.91	23.32
Elongation coefficient, l/s*	1.10	1.65	1.48

Note: * *l* – length, *s* – inclusion thickness.

Table 4. The results of the hot ductility of selected high-Mn steels at the temperature of 1100°C

No.	Steel designation	Chemical composition, (wt%)	RA, %	References
1	18Mn-1.5Al	0.60% C; 18.0% Mn; 1.52% Al; 0.0078% N	12	[16]
2	23Mn-1.5Al	0.66% C; 23.6% Mn; 1.40% Al; 0.0092% N	8	[16]
3	18Mn-0.75Al	0.61% C; 17.7% Mn; 0.75% Al; 0.0087% N	17	[16]
4	21Mn-1.5Al	0.50% C; 21.0% Mn; 1.60% Al; 0.0120% N	20	[17]
5	23Mn-1.5Al-Ti	0.50% C; 23.0% Mn; 1.50% Al; 0.014% Ti	38	[17]
6	18Mn-1.5Al-Ti	0.62% C; 17.9% Mn; 1.53% Al; 0.041% Ti	28	[18]
7	18Mn-1Al-Nb	0.55% C; 18.3% Mn; 1.20% Al; 0.020% Nb	10	[18]
8	18Mn-1.5Al-Ti	0.59% C; 18.1% Mn; 1.52% Al; 0.075% Ti	33	[33]
9	18Mn-1.5Al-V	0.61% C; 18.0% Mn; 1.52% Al; 0.052% V	35	[43]

observed in the 24Mn-3Si-1.5Al-Ti steel (Fig. 8 and Fig. 9). Low value of the elongation factor of 1.48 indicates the effectiveness of the modification of non-metallic inclusions with rare earth metals (Ce, La, Nd) carried out in this steel, which, similarly to the modification with calcium compounds in the ladle process [40, 45], significantly reduces the tendency of non-metallic inclusions to elongate. Non-metallic inclusions revealed in the globular form in the 24Mn-3Si-1.5Al-Ti steel will be difficult to deform in the plastic working process and will not affect the unfavourable increase in the anisotropy of plastic properties.

Of course, the EDS method is not a suitable method for accurate, quantitative assessment of chemical composition, especially nitrogen content. For the analysis of N, the WDS (Wavelength Dispersive Spectrometry) method should be used, which is much more precise than the EDS method, also in the case of light elements. In addition, the WDS method allows you to identify individual spectral lines and precisely analyze their intensity. The EDS method is characterized by a faster measurement speed and is more useful in the qualitative analysis of the tested material. In the case of the analyzed article, this was the main intention. The EDS detector was used to identify the elements present in the tested micro-areas of the samples. In order to minimize possible measurement errors in the microanalysis of the chemical composition using the EDS detector, the tests were carried out on polished samples, additionally using an advanced mixed phi-ro and ZAF correction model in quantitative calculations. In addition, the value of the beam current was set at such a level that the dead time value was within the range of 25-35%. In order to improve the accuracy of the qualitative analysis of the chemical composition in the tested micro-areas of the samples, spectral measurements were made at two different values of the accelerating voltage (20 kV and 7-10 kV). The use of low voltage allows the weak lines of the light elements to become visible.

CONCLUSIONS

Basing on performed research, the following conclusions can be drawn. Examined steels are characterized by high metallurgical purity and show a negligible fraction of non-metallic inclusions. In the 27Mn-4Si-2Al steel, AlN and MnS-AlN-type non-metallic inclusions were identified, regular or elongated in the direction of plastic working. Whereas in the 24Mn-3Si-1.5Al-Ti steel, fine globular sulphides, correctly modified with rare earth elements, were revealed. The morphology of modified (Ce, La, Nd)S-type sulphides, revealed in the 24Mn-3Si-1.5Al-Ti steel, favours production of high strength and ductility sheets with low anisotropy of mechanical properties, especially plastic properties. The 24Mn-3Si-1.5Al-Ti steel shows higher hot ductility. In the temperature range from 1050°C to 1200°C, the reduction in area of this steel decreases from about 90% to approx. 58%, while the reduction in area of the 27Mn-4Si-2Al steel, in the same temperature range, decreases from about 66% to approx. 34%. Higher hot ductility of the 24Mn-3Si-1.5Al-Ti steel results from synergy of the interaction of properly modified non-metallic inclusions with rare earth elements and introduced Ti microaddition. Microaddition of titanium, added into the 24Mn-3Si-1.5Al-Ti steel in a concentration of 0.075%, guaranteeing bonding of the whole nitrogen into stable TiN-type nitrides, eliminated the possibility of AlN-type nitrides and complex MnS-type non-metallic inclusions,

harmful to the hot ductility, to precipitate on austenite grain boundaries.

Acknowledgements

REFERENCES

1. Fonstein N. Advanced high strength sheet steels. Physical metallurgy, design, processing and properties. Springer International Publishing, Switzerland, 2015.

2. Kuziak R., Kawalla R., Waengler S. Advanced high strength steels for automotive industry. Archives of Civil and Mechanical Engineering 2008; 8(2): 103–117.

3. Takahashi M. Development of high strength steels for automobiles. Nippon Steel Technical Report 2003; 88(7): 2–7.

4. Lee S., Lee S-Y., Han J., Hwang B. Deformation bahavior and tensile properties of an austenitic Fe-24Mn-4Cr-0.5C high-manganese steel: Effect of grain size. Materials Science and Engineering A 2019; 742: 334–343.

5. Wesselmecking S., Haupt M., Ma Y., Song W., Hirt G., Bleck W. Mechanism-controlled thermomechanical treatment of high manganese steels. Materials Science and Engineering A 2021; 828: 1–9.

6. Sozańska-Jędrusik L., Mazurkiewicz J., Borek W., Matus K. Carbides analysis of the high strength and low density Fe-Mn-Al-Si steels. Archives of Metallurgy and Materials 2018; 63(1): 265–276.

7. De Cooman B.C., Estrin Y., Kim S.K. Twinning-induced plasticity (TWIP) steels. Acta Materialia 2018; 142: 283–362.

8. Fojt-Dymara G., Opiela M., Borek W. Susceptibility of high-manganese steel to high-temperature cracking. Materials 2022; 15(22): 1–11.

9. Jabłońska M., Śmiglewicz A., Niewielski G. The effect of strain rate on the mechanical properties and microstructure of the high-Mn steel after dynamic deformation tests. Archives of Metallurgy and Materials 2015; 60(2): 123–126.

10. Liu Ch., Shen S., Xie P., Wu C. Deformation behaviors of a Fe-20Mn-3Al-3Si TRIP steel under quasi-static compression and dynamic impact. Materials Characterization 191; 1–10.

11. Pierce D.T., Benzing J.T., Jiménez J.A., Hickel T., Bleskov I., Keum J., Raabe D., Witting J.E. The influence of temperature on the strain-hardening behavior of Fe-22/25/28Mn-3Al-3Si TRIP/TWIP steels. Materialia 2022; 22: 1–12.

12. Opiela M., Fojt-Dymara G., Grajcar A., Borek W. Effect of grain size on the microstructure and strain hardening behavior of solution heat-treated low-C high-Mn steel. Materials 2020; 13(7): 1–13.

13. Frommeyer G., Brüx U., Neumann P. Supra-ductile and high-strength manganese TRIP/TWIP steels for high energy absorption purposes. ISIJ International 2003; 43(3): 438–446.

14. Allain S., Chateau J.P., Bouaziz O. A physical model of the twinning-plasticity effect in a high manganese austenitic steel. Materials Science and Engineering A 2004; 387: 143–147.

15. Kim J.K., Chen L., Kim H.S., Kim S.K., Estrin Y., De Cooman B.C. On the tensile behavior of high-manganese twinning-induced plasticity steel. Metallurgical and Materials Transactions A 2009; 40: 3147–3158.

16. Liu H., Liu J., Wu B., Shen Y., He Y., Su X. Effect of Mn and Al contents on hot ductility of high alloy Fe-xMn-C-yAl austenite TWIP steels. Materials Science and Engineering A 2017; 708: 360–374.

17. Mejia I., Salas-Reyes A.E., Calvo J., Cabrera J.M. Effect Ti and B microadditions on the hot ductility behavior of a high-Mn austenitic Fe-23Mn-1.5Al-1.3Si-0.5C TWIP steel. Materials Science and Engineering A 2015; 648: 311–329.

18. Kang S.E., Banerjee J.R., Maina E.M., Mintz B. Influence of B and Ti on hot ductility of high Al and high Al, Nb containing TWIP steels. Materials Science and Technology 2013; 29: 1225–1232.

19. Liu H., Liu J., Michelic S.K., Shen S., Su X., Wu B., Dinh H. Characterization and analysis of non-metallic inclusions in low carbon Fe-Mn-Si-Al TWIP steels. Steel Research International 2016; 87: 1723–1732.

20. Li D., Feng Y., Song S., Liu Q., Bai Q., Wu G., Ren F. Influence of Nb-microalloying on microstructure and mechanical properties of Fe-25Mn-3Si-3Al TWIP steel. Materials and Design 2015; 84: 238–244.

21. Park J.H., Kim D-J., Min D.J. Characterization of nonmetallic inclusions in high-manganese and aluminium-alloyed austenitic steels. Metallurgical and Materials Transactions A 2012; 43(7): 2316–2324.

22. Wang Y-N., Yang J., Wang R-Z., Xin X-L., Xu L-Y. Effects of non-metallic inclusions on hot ductility of high manganese TWIP steels containing different aluminium contents. Metallurgical and Materials Transactions B 2016; 47: 1697–1712.

23. Hamada A.S., Karjalainen I.P. Hot ductility behaviour of high-Mn TWIP steels. Materials Science and Engineering A 2011; 528: 1819–1827.

24. Jang J-M., Kim S-J., Kang N.H., Cho K.M., Suh D.W. Effect of annealing conditions on microstructure and mechanical properties of low carbon, manganese transformation-induced plasticity steel. Met-

als and Materials International 2009; 15: 909–916.

25. Kim J., Lee S-J., De Cooman B.C. Effect of Al on the stacking fault energy of Fe-18Mn-0.6C twinning-induced plasticity. Scripta Materialia 2011; 65: 363–366.

26. Mintz B. The influence of composition on the hot ductility of steels and to the problem of transverse cracking. ISIJ International 1999; 39: 833–855.

27. Mintz B., Yue S., Jonas J.J. Hot ductility of steels and its relationship to the problem of transverse cracking during continuous casting. International Materials Reviews 1991; 36: 187–217.

28. Kang S.E., Tuling A., Banerjee J.R., Gunawarnada W.D, Mintz B. Influence of B on hot ductility of high Al, TWIP steels. Materials Science and Technology 2011; 27: 95–100.

29. Kang S.E., Banerjee J.R., Mintz B. Influence of S and AlN on hot ductility of high Al, TWIP steels. Materials Science and Technology 2012; 28: 589–596.

30. Kang S.E., Banerjee J.R., Mintz B. The hot ductility of Nb/V containing high Al, TWIP steels. Materials Science and Technology 2011; 27: 909–915.

31. Kang S.E., Banerjee J.R., Tuling A. Influence of P and N on hot ductility of high Al, boron containing TWIP steels. Materials Science and Technology 2014; 30: 1328–1335.

32. Abushosha R., Comineli O., Mintz B. Influence of Ti on hot ductility of C-Mn-Al steels. Materials Science and Technology 1999; 15: 278–286.

33. Qaban A., Mintz B., Kang S.E., Naher S. Hot ductility of high Al TWIP steels containing Nb and Nb-V. Materials Science and Technology 2017; 33: 1645–1656.

34. Gigacher G., Krieger W., Scheler P.R., Thomser C. Non-metallic inclusions in high-manganese steels. Steel Research International 2005; 76(9): 644–649.

35. Grässel O., Frommeyer G., Derder C., Hofmann H. Phase transformation and mechanical properties of Fe-Mn-Si-Al TRIP steels. Journal Physique 1997; 7: 338–388.

36. Grässel O., Kruger L., Frommeyer G., Meyer L.W. High-strength Fe-Mn-(Al,Si) TRIP/TWIP steels development – properties – application. International Journal of Plasticity 2000; 16: 391–1409.

37. Pichler A., Stiaszny P. TRIP steel with reduced silicon content. Steel Research 1999; 70(11): 459–465.

38. Frommeyer G., Brüx U. Microstructures and mechanical properties of high-strength Fe-Mn-Al-Si light-weight TRIPLEX steels. Steel Research International 2006; 77(9–10): 627–633.

39. Abushosha R., Ayyad S., Mintz B. Influence of cooling rate and MnS inclusions on the hot ductility of steels. Materials Science and Technology 1998; 14: 227–235.

40. Opiela M., Grajcar A. Modification of non-metallic inclusions by rare-earth elements in microalloyed steels. Archives of Foundry Engineering 2012; 12(2): 129–134.

41. Mintz B., Qaban A. The influence of precipitation, high levels of Al, Si, P and a small B addition on the hot ductility of TWIP and TRIP assisted steels: A critical review. Metals 2022; 12(3): 1–31.

42. Borrmann L., Senk D., Steenken B., Rezende J. Influence of cooling and strain rates on the hot ductility of high manganese steels within the system Fe-Mn-Al-C. Steel Research International 2020; 92(2): 1–10.

43. Kang S.E., Kang M.H., Mintz B. Influence of vanadium, boron and titanium on hot ductility of high Al TWIP steels. Materials Science and Technology 2020; 37: 42–58.

44. Osinkolu G.A., Tacikowski M., Kobylanski A. Combined effect of AlN and sulphur on hot ductility of high purity iron-base alloys. Materials Science and Technology 1985; 1: 520–525.

45. Fojt-Dymara G., Opiela M. Hot ductility behavior of Fe-0.05C-24Mn-3.5Si-1.6Al steel with Nb and Ti microadditions. International Journal of Modern Manufacturing technologies 2022; 2: 319–328.